

## Research Article

# A Dynamic Method to Predict the Earthquake-Triggered Sliding Displacement of Slopes

Wenkai Feng,<sup>1</sup> Zhichun Lu,<sup>2,3</sup> Xiaoyu Yi,<sup>1</sup> and Shan Dong<sup>1,2</sup> 

<sup>1</sup>State Key Laboratory of Geohazard Prevention and Geoenvironment Protection (Chengdu University of Technology), Chengdu 610059, China

<sup>2</sup>Three Gorges Research Center for Geohazards, China University of Geosciences, Wuhan 430074, China

<sup>3</sup>Faculty of Engineering, China University of Geosciences, Wuhan 430074, China

Correspondence should be addressed to Shan Dong; dongshan1994@hotmail.com

Received 11 October 2021; Revised 29 October 2021; Accepted 30 October 2021; Published 15 November 2021

Academic Editor: Gan Feng

Copyright © 2021 Wenkai Feng et al. This is an open access article distributed under the Creative Commons Attribution License, which permits unrestricted use, distribution, and reproduction in any medium, provided the original work is properly cited.

The earthquake-induced permanent displacement is an important index of the potential damage to a slope during an earthquake. The Newmark method assumes that a slope is a rigid-plastic body, and the seismic responses of sliding masses or seismic forces along the slide plane are ignored. The decoupled method considers no relative displacement across the sliding plane, so it overpredicts the seismic response of the sliding mass. Both dynamic and sliding analyses are performed in the coupled method, but when  $T_s/T_m$  is large, the results are unconservative. In this paper, a method is proposed to predict the earthquake-triggered sliding displacement of slopes. The proposed method is based on the Newmark rigid method, coupled method, and decoupled method considering both the forces at the sliding interface and the system dynamics under critical conditions. For the flexible system, the displacements are calculated with different stiffness values, and the results show that as the stiffness increases and tends to infinity, the critical acceleration and displacements of the proposed method are close to those of the Newmark method. The proposed method is also compared with the Newmark method with the period ratio  $T_s/T_m$ . At small values of  $T_s/T_m$ , the flexible system analysis results of the displacement are more conservative than those of the rigid block model; at larger values of  $T_s/T_m$ , the rigid block model is more conservative than the flexible system.

## 1. Introduction

An earthquake can trigger a number of geotechnical failures, including liquefaction, the collapse of loose deposits, landslides, rock falls, rock avalanches, and landslide dams. Among these events, landslides are highly damaging [1]. Earthquakes with magnitudes greater than 4.0 can trigger landslides on very susceptible slopes, and earthquakes with magnitudes greater than 6.0 can generate widespread landslides [2]. Permanent sliding displacement represents a common damage parameter used to evaluate the seismic stability of slopes. This displacement represents the cumulative downslope movement of a sliding mass due to earthquake shaking. The magnitude of sliding displacement has been correlated with the seismic performance of slopes [3]. Thus, the earthquake-induced sliding displacement of a

system must be assessed in evaluations of earthquake-induced landslides [4].

The stability of slopes subjected to earthquakes can be evaluated in several ways. The simplest approach is the pseudostatic analysis method proposed by Terzaghi [5]. This strategy consists of generalizing the classical limit equilibrium method to the dynamic case; the equilibrium of the most important soil volume is assessed by assuming that seismic acceleration is represented by a static force. In pseudostatic analysis, the soil is assumed to be rigid; as a result, this formulation tends to yield conservative results [6, 7]. In fact, many slopes have experienced earthquake accelerations well above the yield thresholds but suffered little or no permanent displacement [8]. Conversely, because pseudostatic analysis is very inaccurate, slopes can be unstable at safety factors greater than 1 [5, 9, 10]. Another

limitation of the pseudostatic approach is the lack of information regarding permanent displacement. Given the above considerations, the Newmark method [11] was proposed as a simplified and reliable method of assessing seismic slope stability and calculating permanent displacement. The Newmark method analyses the dynamics of a rigid block sliding on a flat rough surface under earthquake shaking motion. The Newmark method uses two parameters associated with the yield acceleration and acceleration time history of the rigid foundation. The critical acceleration is defined as that acceleration at which the ground motion creates a destabilizing force sufficient to temporarily reduce the safety factor of the slope to less than 1, and sliding begins when the shear force at the contact surface exceeds the shear strength. Then, the relative velocity between the rigid block and foundation is integrated to calculate the relative sliding displacement.

Given its simplicity and reliability, the Newmark method has been widely used; however, the major limitation of this method is that the sliding mass is considered a rigid block. Makdisi and Seed [12] modified the Newmark procedure and performed a dynamic analysis of a rigid block. However, the modified Newmark procedure does not accurately model the force at the sliding interface because the sliding motion of the sliding mass is ignored. The decoupled method is generally overconservative or slightly unconservative. The nonlinear coupled stick-slip deformable sliding model was proposed by Rathje and Bray [13] for horizontal directional sliding. Compared to the rigid sliding block model, the nonlinear coupled stick-slip deformable sliding block model offers a more realistic representation of the dynamic response of an earth/waste structure by accounting for the deformability of the sliding mass and considering the simultaneous occurrence of a nonlinear dynamic response and periodic sliding episodes. Many researchers have also proposed displacement prediction methods. For example, Ambrasey and Menu [14] used 50 strong ground motion records from 11 worldwide earthquakes and proposed a sliding displacement predictive model based on Newmark rigid block analysis and found that the  $k_y/PGA$  ratio has a large influence on the sliding displacement of earthquake-triggered landslides. Qi [15] proposed an algorithm for the seismic permanent displacement of a rock slope considering the degradation law of the structural plane undulant angle. Zafarani and Soghrat [16] proposed an empirical prediction equation based on the peak ground acceleration (PGA) obtained in different parts of Iran. Jafarian et al. [17] proposed and developed an empirical model based on regression analyses. Dong et al. [18] proposed the calculation method of landslide displacement considering the deterioration effect of structural plane.

In this paper, a method is proposed to predict the earthquake-triggered sliding displacement of slopes. The proposed method for determining the earthquake-triggered sliding displacement of a slope is based on the coupled and Newmark methods. The procedures and dynamics of the stick and slip phases are studied to estimate the earthquake-triggered sliding displacement of landslides. The slope

sliding mass is considered a lumped mass system, and the ground motion is considered horizontal. Dynamic analyses are performed based on the mechanical equilibrium equation under critical conditions to define the slope from stick to slip. The proposed method is compared with the Newmark rigid block method.

## 2. Previous Work

**2.1. Newmark Method.** To consider seismic conditions in slope stability analyses, Newmark [11] proposed the Newmark sliding rigid block method. The Newmark method [11] is a simplified formulation for seismic soil slope stability analysis that considers rigid block sliding on an inclined flat frictional surface.

**2.1.1. Assumptions of the Newmark Method.** The common assumptions and limitations of Newmark's method are as follows [11, 19]:

- (1) The landslide is a rigid plastic body, and the mass does not deform internally, does not experience permanent displacement at accelerations below the critical (yield) level, and deforms plastically along a discrete basal shear surface when the critical acceleration is exceeded
- (2) The static and dynamic shearing resistance of the soil are equal and constant
- (3) No pore water pressure variations are considered
- (4) The critical acceleration is not strain dependent and thus remains constant throughout the analysis
- (5) The upslope resistance to sliding is assumed to be infinitely large, such that upslope displacement is prohibited

**2.1.2. Critical Acceleration.** This rigid block is subjected to the same seismic accelerations that occur during actual slope instability events. Therefore, when the static and dynamic forces exceed the shear strength of the sliding surface,  $F_s$  is reduced to 1.0, and the block is displaced. The critical acceleration can be defined as the minimum seismic acceleration required to overcome the shear resistance and initiate the displacement of the rigid block. Thus, critical acceleration is the most significant parameter and must be estimated first. In the Newmark method, the critical acceleration is exceeded when the inertial force acts in the downslope direction; therefore, resolving forces perpendicular to the inclined plane gives

$$FS_d = \frac{\text{available resisting force}}{\text{pseudostatic driving force}} = \frac{[\cos \beta - k_y \sin \beta] \tan \phi}{\sin \beta + k_y \cos \beta}. \quad (1)$$

The yield acceleration is the minimum pseudostatic acceleration required to produce block instability.

$$\begin{aligned} k_y &= \tan(\Phi - \beta), \\ a_c &= k_y g, \end{aligned} \quad (2)$$

where  $a_c$  is the critical acceleration,  $k_y$  is the yield coefficient,  $g$  is the acceleration due to gravity,  $\Phi$  is the friction angle between the block and the plane,  $\beta$  is the slope angle, and  $F_s$  is the safety factor.

**2.1.3. Newmark Displacement.** The Newmark displacement is the permanent sliding displacement experienced by the block when shaking with an acceleration that exceeds the critical value given by the above equation. Such a displacement can be obtained by the double time integration of the intervals of the excitation accelerogram which are above  $a_c$  (Figure 1). Notably, the segments that are below the bound (i.e.,  $a_c$ ) do not generate any displacement, given that they correspond to uphill acceleration.

**2.2. Decoupled Method.** Rathje and Bray [21] proposed a decoupled method that was modified from a generalized SDOF system with the mass and stiffness distributed along the height of the system. The mode shape in the decoupled method was introduced by considering the boundary condition for a horizontal deposit with a constant shear-wave velocity profile [9]. The governing equation of motion for the SDOF system is

$$\mathbf{M}\ddot{\mathbf{Y}}_1 + 2\lambda\omega_1\dot{\mathbf{Y}}_1 + \omega_1^2\mathbf{Y}_1 = -\frac{\mathbf{L}_1}{\mathbf{M}_1} \cdot \ddot{u}_g(t), \quad (3)$$

where  $Y_1$  is the modal coordinate,  $u_g(t)$  is the input ground motion,  $\lambda$  is the viscous material damping ratio,  $M_1$  is the generalized mass distributed along the height of the system,  $L_1$  is a mode shape term defining ground acceleration in the direction of the height of the system, and  $\omega_1$  is a natural circular frequency associated with the fundamental period of the system.

Chopra and Zhang proposed the yield-equivalent base acceleration considering the acceleration profile of the system:

$$\text{HEA}(t) = \frac{\mathbf{L}_1}{\mathbf{M}} \ddot{\mathbf{Y}}_1 + \ddot{u}_g(t), \quad (4)$$

where  $M$  is the total mass of the soil deposit layer.

The equivalent acceleration time history is used as input acceleration in Newmark rigid block analysis to obtain the permanent displacement as follows:

$$\ddot{s} = -k_y g - \text{HEA}(t) = -k_y g - \frac{\mathbf{L}_1}{\mathbf{M}} \ddot{\mathbf{Y}}_1 - \ddot{u}_g(t). \quad (5)$$

### 2.3. Coupled Analysis

**2.3.1. Stick Phase.** In coupled analysis [13], the dynamic response of the sliding mass and the permanent displacement are modelled together so that the effect of the plastic sliding displacement on ground motion is

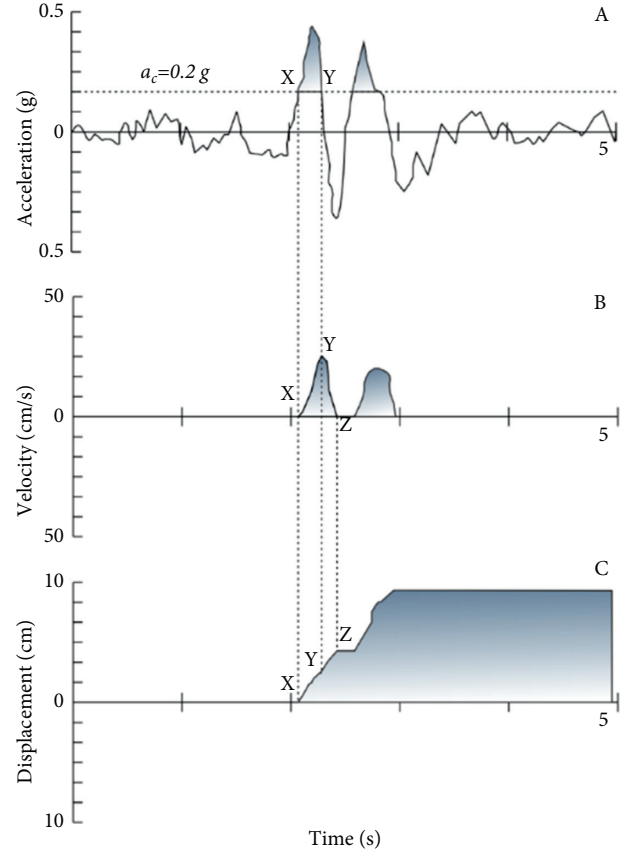


FIGURE 1: The Newmark integration algorithm (adapted from Kramer [20]). The strong-motion record having a hypothetical  $a_c$  of 0.2 g is superimposed. To the left of point X accelerations are less than  $a_c$ , and there is no displacement. To the right of point X those parts of the strong-motion record lying above  $a_c$  are integrated over time to derive a velocity profile of the block. Integration begins at point X and the velocity increases to point Y, the maximum velocity for this pulse. Past point Y the ground acceleration drops below  $a_c$ , but the block continues to move because of its inertia. Friction and ground motion in the opposite direction cause the block to decelerate until it stops at point Z. All pulses of the ground motion exceeding  $a_c$  are integrated to yield a cumulative displacement profile of the landslide block.

considered. The governing equation of the dynamic equilibrium of a multiple degree-of-freedom (MDOF) lumped mass system is given by

$$\mathbf{M}\ddot{\mathbf{u}} + \mathbf{C}\dot{\mathbf{u}} + \mathbf{K}\mathbf{u} = -\mathbf{M} \cdot \mathbf{1} \cdot \ddot{u}_g, \quad (6)$$

where  $M$ ,  $C$ ,  $K$ ,  $\ddot{u}$ ,  $\dot{u}$ ,  $u$ , and  $\ddot{u}_g$  are the mass matrix, damping matrix, stiffness matrix, vector of the nodal relative accelerations, vector of the nodal relative velocities, vector of the nodal relative displacements, and the acceleration time history, respectively.

**2.3.2. Slip Phase.** When the force at the base of the sliding mass exceeds the frictional strength at the sliding mass/foundation interface for sliding in the positive direction, the following scalar equation can be obtained:

$$-M_T \ddot{u}_g - 1^T \mathbf{M} \cdot \ddot{\mathbf{u}} = u M_T g, \quad (7)$$

where  $M_T \ddot{u}_g$  is the force due to the ground acceleration,  $1^T \mathbf{M} \cdot \ddot{\mathbf{u}}$  is the force at the sliding interface from the non-uniform acceleration profile within the sliding mass, and  $u M_T g$  is the frictional resistance at the sliding interface.

After sliding is initiated, the excitation at the base is the acceleration of the ground and the acceleration associated with the sliding displacement. The governing equation is

$$\mathbf{M} \ddot{\mathbf{u}} + \mathbf{C} \dot{\mathbf{u}} + \mathbf{K} \mathbf{u} = -\mathbf{M} \cdot \mathbf{1} \cdot (\ddot{s} + \ddot{u}_g), \quad (8)$$

where  $\ddot{s}$  is the sliding acceleration at the base of the sliding mass. During sliding, the equilibrium at the shear interface is represented as follows:

$$-M_T (\ddot{s} + \ddot{u}_g) - 1^T \mathbf{M} \cdot \ddot{\mathbf{u}} = u M_T g. \quad (9)$$

Combined with the above equation, the vector of the nodal acceleration during sliding is used to calculate the sliding acceleration at the base of the sliding mass with

$$\begin{aligned} m_1 \ddot{u}_1 - (\dot{u}_2 - u_1) c_2 + \dot{u}_1 c_1 - (u_2 - u_1) k_2 + u_1 k_1 - m_1 g \sin \theta &= m_1 \ddot{u}_g \cos \theta \\ &\dots \\ m_{n-1} \ddot{u}_{n-1} - (\dot{u}_n - u_{n-1}) c_n + (\dot{u}_{n-1} - u_{n-2}) c_{n-1} - (u_n - u_{n-1}) k_n + (u_{n-1} - u_{n-2}) k_{n-1} - m_{n-1} g \sin \theta &= m_{n-1} \ddot{u}_g \cos \theta \\ m_n \ddot{u}_n + (\dot{u}_n - u_{n-1}) c_n + (u_n - u_{n-1}) k_n - m_n g \sin \theta &= m_n \ddot{u}_g \cos \theta. \end{aligned} \quad (11)$$

Rearranging the equations yields the following relational expression:

$$\begin{aligned} m_1 \ddot{u}_1 + (c_1 + c_2) \dot{u}_1 - c_2 \dot{u}_2 + (k_1 + k_2) u_1 - k_2 u_2 &= m_1 \ddot{u}_g \cos \theta + m_1 g \sin \theta \\ &\dots \\ m_{N-1} \ddot{u}_{n-1} - c_{n-1} \dot{u}_{n-2} + (c_{n-1} + c_n) \dot{u}_{n-1} - c_n \dot{u}_n - k_{n-1} u_{n-2} + (k_{n-1} + k_n) u_{n-1} - k_n u_n &= m_{n-1} \ddot{u}_g \cos \theta + m_{n-1} g \sin \theta \\ m_n \ddot{u}_n - c_n \dot{u}_{n-1} + c_n \dot{u}_n - k_n u_n - k_n u_{n-1} &= m_n \ddot{u}_g \cos \theta + m_n g \sin \theta. \end{aligned} \quad (12)$$

These scalar equations can be combined to form a single  $N \times N$  matrix equation:

$$\mathbf{M} \ddot{\mathbf{u}} + \mathbf{C} \dot{\mathbf{u}} + \mathbf{K} \mathbf{u} = \mathbf{M} \cdot \mathbf{1} (\ddot{u}_g \cdot \cos \theta + g \sin \theta), \quad (13)$$

where  $M$ ,  $C$ , and  $K$  are the mass matrix, damping matrix, and stiffness matrix, respectively. The damping matrix  $C$  is generated by a Rayleigh model as  $\mathbf{C} = \alpha \mathbf{M} + \beta \mathbf{K}$ . Additionally,  $\ddot{u}_g$  is the acceleration time history at the slope base;  $\theta$  is the slope angle;  $\ddot{\mathbf{u}}$  is the vector of nodal relative

$$\ddot{s} = -u g - \frac{1}{M_T} 1^T \mathbf{M} \cdot \ddot{\mathbf{u}} - \ddot{u}_g. \quad (10)$$

### 3. The Proposed Method

In the proposed method, the direction of the ground motion is assumed to be contrary to the sliding direction. Because sliding in the uphill direction occurs only when the slope angle and friction angle are small (approaching level), this paper mainly considers sliding in the downslope direction.

**3.1. Stick Condition.** In this paper, a lumped mass system is considered, and the acceleration is considered horizontal (Figures 2 and 3). In the improved method, the processes consist of two phases, namely, stick and slip phases. Under stick conditions, the motion of each lumped mass in the parallel direction is described by the following ordinary differential equations:

accelerations;  $\ddot{\mathbf{u}}$  is the vector of nodal relative velocities; and  $\mathbf{u}$  is the vector of nodal relative displacements.

**3.2. Critical Condition.** The critical condition is considered when the available resisting force is equal to the driving force. When the inertial force acts in the downslope direction, the resolving forces perpendicular to the inclined plane can be formulated as follows:

$$F_s = \frac{\text{available resisting force}}{\text{driving force}} = \frac{N \cdot \tan \phi}{1^T \cdot \mathbf{M} \cdot \ddot{\mathbf{u}} + 1^T \cdot \mathbf{M} \cdot \mathbf{1} \cdot \ddot{u}_g \cos \theta + 1^T \cdot \mathbf{M} \cdot \mathbf{1} \cdot g \sin \theta}. \quad (14)$$

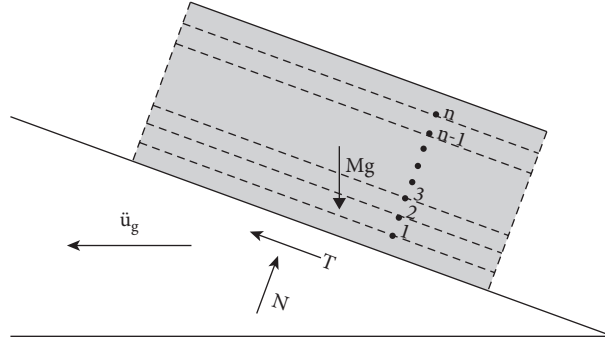


FIGURE 2: Schematic diagram of the system. The figure displays a block on an inclined plane with a slope characterized by an angle  $\theta$ .  $T$  and  $N$  are the parallel (shear) and orthogonal (normal) reaction forces, respectively.

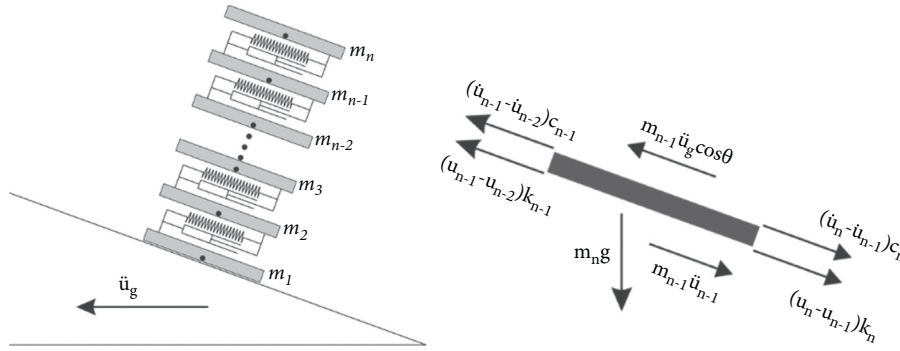


FIGURE 3: Mechanical analysis of the sliding mass during the sliding phase.

Distribution of forces perpendicular to the slope is

$$\mathbf{1}^T \cdot \mathbf{M} \cdot \mathbf{1} \cdot \ddot{u}_g \sin \theta = \mathbf{g} \cdot \mathbf{1}^T \cdot \mathbf{M} \cdot \mathbf{1} \cdot \cos \theta - N. \quad (15)$$

The critical acceleration can be obtained when  $F_s$  equals 1.0:

$$a_c = g \tan(\varnothing - \theta) - \frac{\mathbf{1}^T \cdot \mathbf{M} \cdot \ddot{u}}{\mathbf{1}^T \cdot \mathbf{M} \cdot \mathbf{1} \cdot \cos \theta \cdot (1 + \tan \varnothing \cdot \tan \theta)}, \quad (16)$$

where  $c$  is the cohesive force,  $N$  is the supporting force below the sliding surface,  $\varnothing$  is the friction angle, and  $\ddot{u}$  is the vector of nodal relative accelerations in the stick phase.

**3.3. Slip Condition.** When the slope is excited by seismic forces, the mass begins to slide; this is the second (slip) phase. In this phase, the acceleration of the ground motion and the acceleration associated with the sliding displacement are considered. The matrix equation is as follows:

$$\mathbf{M}\ddot{u} + \mathbf{C}\dot{u} + \mathbf{K}u = \mathbf{M} \cdot \mathbf{1} \cdot (\ddot{u}_g \cdot \cos \theta - \ddot{s} + g \sin \theta), \quad (17)$$

where  $\ddot{s}$  is the sliding acceleration at the base of the sliding mass ( $\ddot{s}$  should be larger than  $\ddot{u}$ ).

During sliding, the equilibrium at the shear interface is

$$\begin{aligned} & -\mathbf{1}^T \cdot \mathbf{M} \cdot \mathbf{1} \cdot \ddot{u}_g \cos \theta + \mathbf{1}^T \cdot \mathbf{M} \cdot \mathbf{1} \cdot \ddot{s} + \mathbf{1}^T \cdot \mathbf{M} \cdot \ddot{u} \\ & = -(\mathbf{1}^T \cdot \mathbf{M} \cdot \mathbf{1} \cdot g \cos \theta - \mathbf{1}^T \cdot \mathbf{M} \cdot \mathbf{1} \cdot \ddot{u}_g \sin \theta) \cdot \tan \varnothing \\ & \quad + \mathbf{1}^T \cdot \mathbf{M} \cdot \mathbf{1} \cdot g \sin \theta. \end{aligned} \quad (18)$$

The formulations in (17) and (18) can be combined to obtain the following formula:

$$\mathbf{M}^* \ddot{u} + \mathbf{C}\dot{u} + \mathbf{K}u = \mathbf{M} \cdot \mathbf{1} \cdot [g(\cos \theta - \ddot{u}_g \sin \theta) \cdot \tan \varnothing]. \quad (19)$$

In this equation,  $M^*$  is defined as follows:

$$\mathbf{M}^* = \mathbf{M} - \frac{1}{\mathbf{1}^T \mathbf{M} \mathbf{1}} \cdot \mathbf{M} \mathbf{1} \mathbf{1}^T \mathbf{M}. \quad (20)$$

$\ddot{s}$  is defined as follows:

$$\ddot{s} = -(g \cos \theta - \ddot{u}_g \sin \theta) \tan \varnothing - \frac{1}{\mathbf{1} \cdot \mathbf{M} \cdot \mathbf{1}^T} \cdot \mathbf{1}^T \cdot \mathbf{M} \cdot \ddot{u} + \ddot{u}_g \cos \theta + g \sin \theta. \quad (21)$$

Under slip conditions,  $M^*$ , as defined in (20), is only used in the case with 1 or 2 DOFs. When the system has

more than 2 DOFs, a new approach must be considered. These  $N + 1$  equations can be arranged as follows:

$$\begin{aligned} -\mu N + (m_b + 1^T \mathbf{M} \mathbf{1}) g \sin \theta &= -(m_b + 1^T \mathbf{M} \mathbf{1}) (\ddot{u}_g \cdot \cos \theta - \ddot{s}) + 1^T \mathbf{M} \ddot{u}, \\ \mathbf{M} \ddot{\mathbf{d}} + \mathbf{C} \dot{\mathbf{d}} + \mathbf{K} \mathbf{d} &= \mathbf{M} \mathbf{1} (\ddot{u}_g \cdot \cos \theta - \ddot{s} + g \sin \theta). \end{aligned} \quad (22)$$

Some previous researchers have circumvented this problem by assigning a mass directly to the sliding surface [22, 23]. In the computer code (MATLAB) developed for this analysis, only half of the mass of the base element is assigned to the lumped mass for that element, and the other half is assigned to the sliding interface. This approach assures that  $1^T \cdot \mathbf{M} \cdot 1$  is not equal to the sum of the lumped mass, and therefore,  $M^*$  cannot be singular.

#### 4. Discussion

**4.1. Rigid Block.** Using the classical Newmark method considered under slip conditions, block sliding is obtained by integrating the part of the input acceleration that exceeds the critical level ( $\ddot{u}_g - g \tan(\phi - \theta)$ ). Actually, the situation involves a relevant simplifying condition that is different from the proposed method in this paper. When the model is considered a rigid block, the details of the proposed method are as follows.

**4.1.1. Stick Condition.** The equation of motion of the block in parallel to the slope is

$$Mg \cdot \sin \theta - \tan \varnothing \cdot N = -M \cdot \ddot{u}_g \cdot \cos \theta. \quad (23)$$

The equation of motion of the block in the orthogonal directions is as follows:

$$Mg \cdot \cos \theta - N = M \cdot \ddot{u}_g \cdot \sin \theta. \quad (24)$$

**4.1.2. Critical Condition.** For the rigid block model, the critical acceleration is the same as the Newmark method. The yield acceleration is the minimum pseudostatic acceleration required to produce instability of the block. The critical acceleration is as follows:

$$F_s = \frac{\text{available resisting force}}{\text{driving force}} = \frac{N \cdot \tan \varnothing}{1^T \cdot M \cdot \ddot{u} + 1^T \cdot M \cdot 1 \cdot \ddot{u}_g \cos \theta + 1^T \cdot M \cdot 1 \cdot g \sin \theta}. \quad (30)$$

$$\begin{aligned} k_y &= \tan(\varnothing - \theta), \\ a_c &= k_y g. \end{aligned} \quad (25)$$

**4.1.3. Slip Condition.** The equation of motion of the block in parallel to the slope is

$$Mg \cdot \sin \theta - \tan \varnothing \cdot N = -M \cdot (\ddot{u}_g \cdot \cos \theta - \ddot{s}). \quad (26)$$

The equation of motion of the block in the orthogonal directions is as follows:

$$Mg \cdot \cos \theta - N = M \cdot \ddot{u}_g \cdot \sin \theta. \quad (27)$$

$\ddot{s}$  should be

$$\begin{aligned} \ddot{s} &= g \cdot \sin \theta - \tan \varnothing \cdot g \cdot \cos \theta + \tan \varnothing \cdot \ddot{u}_g \cdot \sin \theta + \ddot{u}_g \\ &\quad \cdot \cos \theta. \end{aligned} \quad (28)$$

**4.2. Sliding in the Uphill Direction.** The sliding in the uphill direction occurs only when the slope angle and friction angle are small (approaching level). The equations are as follows.

**4.2.1. Stick Condition.** When in the stick condition, the scalar equations can be combined in a single  $N \times N$  matrix equation as

$$\mathbf{M} \ddot{\mathbf{d}} + \mathbf{C} \dot{\mathbf{d}} + \mathbf{K} \mathbf{d} = -\mathbf{M} \mathbf{1} (\ddot{u}_g \cos \theta - g \sin \theta). \quad (29)$$

**4.2.2. Critical Condition.** When the inertial force acts in the uphill direction, the resolving forces perpendicular to the inclined plane are given as follows:

Distribution of forces perpendicular to the slope is

$$-1^T \cdot M \cdot 1 \cdot \ddot{u}_g \sin \theta = g \cdot 1^T \cdot M \cdot 1 \cdot \cos \theta - N. \quad (31)$$

The critical acceleration was obtained when  $F_s$  is equal to 1.0.

$$a_c = -g \tan(\varnothing - \theta) + \frac{1^T \cdot M \cdot \ddot{u}}{1^T \cdot M \cdot 1 \cdot \cos \theta \cdot (1 + \tan \varnothing \cdot \tan \theta)}. \quad (32)$$

4.2.3. *Slip Condition.* The matrix equation is as follows:

$$\mathbf{M}\ddot{\mathbf{u}} + \mathbf{C}\dot{\mathbf{u}} + \mathbf{K}\mathbf{u} = -\mathbf{M} \cdot 1 \cdot (\ddot{u}_g \cdot \cos \theta + \ddot{s} - g \sin \theta), \quad (33)$$

where  $\ddot{s}$  is the sliding acceleration at the base of the sliding mass ( $\ddot{s}$  should be larger than  $\ddot{u}$ ).

During sliding, the equilibrium at the shear interface is

$$\begin{aligned} & 1^T \cdot \mathbf{M} \cdot 1 \cdot \ddot{u}_g \cos \theta + 1^T \cdot \mathbf{M} \cdot 1 \cdot \ddot{s} + 1^T \cdot \mathbf{M} \cdot \ddot{u} \\ & = -(1^T \cdot \mathbf{M} \cdot 1 \cdot g \cos \theta + 1^T \cdot \mathbf{M} \cdot 1 \cdot \ddot{u}_g \sin \theta) \cdot \tan \varnothing \\ & + 1^T \cdot \mathbf{M} \cdot 1 \cdot g \sin \theta. \end{aligned} \quad (34)$$

Combining with the formulations of (33) and (34),

$$\mathbf{M}^* \ddot{\mathbf{u}} + \mathbf{C}\dot{\mathbf{u}} + \mathbf{K}\mathbf{u} = \mathbf{M} \cdot 1 \cdot [(g \cos \theta + \ddot{u}_g \sin \theta) \cdot \tan \varnothing], \quad (35)$$

where  $M^*$  is defined as follows:

$$\mathbf{M}^* = \mathbf{M} - \frac{1}{1^T \mathbf{M} 1} \cdot \mathbf{M} 1 1^T \mathbf{M}. \quad (36)$$

$\ddot{s}$  is defined as

$$\ddot{s} = -(g \cos \theta + \ddot{u}_g \sin \theta) \tan \varnothing - \frac{1}{1 \cdot \mathbf{M} \cdot 1^T} \cdot 1^T \cdot \mathbf{M} \cdot \ddot{u} - \ddot{u}_g \cos \theta + g \sin \theta. \quad (37)$$

## 5. Example and Comparison

5.1. *Example.* To verify the validity and feasibility of this method, a simple case is chosen with an approximate sliding mass thickness of 8 m. When the slope in the stick phase is considered, it has 16 degrees of freedom. The parameters include a slope angle of  $15^\circ$ , a friction angle of  $25^\circ$ , and a unit weight of  $20 \text{ kN/m}^3$ . The Cholame-Shandon Array #5 record from the 1966 Parkfield earthquake ( $M_w = 6.69$ ) was used in this simple case. In this example, the rigid block is calculated by the proposed method and the Newmark method. Figures 4 and 5 show that the sliding displacement of the proposed method is larger than that of the classical Newmark method. The Newmark displacement is 0.016 m, while the rigid block model in the proposed model is 0.177 m.

In addition, the flexible model is also calculated by computer code (MATLAB). In the flexible model, the critical acceleration obtained from the proposed method is not constant because the dynamics under critical conditions are considered. This approach should be more accurate than using the yield acceleration of the Newmark method. The procedure and the results of the proposed flexible method are shown in Figure 6. The displacements of the method proposed in this paper are 0.025 m, and the results are larger than the rigid block model.

### 5.2. Comparison

5.2.1. *Comparison of the Proposed Flexible System Analysis with the Newmark Method.* The coupled and decoupled methods are mainly aimed at the horizontal earth structure. The critical acceleration is the same as the Newmark critical acceleration. In this paper, the proposed method is compared with the Newmark method. The Newmark method

assumes that the slope is a rigid-plastic body. Furthermore, the mass does not deform internally, does not experience a permanent displacement at accelerations below the critical or yield level, and deforms plastically along a discrete basal shear surface when the critical acceleration is exceeded. The results of the proposed method are calculated with different stiffness values, and the results of the proposed method are compared with the Newmark method; the results are shown in Figures 7 and 8.

In Figure 7, the critical accelerations are compared; in the Newmark rigid block method, the value of the critical acceleration is constant. Because the stiffness increases, the fluctuations in the vector of nodal relative accelerations decrease. As the stiffness increases, the critical acceleration obtained from the proposed method is close to the Newmark critical acceleration.

Figure 8 shows the displacement results. For small stiffness values, the displacements obtained with the proposed method and Newmark method display a large difference. As the stiffness increases, this difference in displacements decreases, and, at very large stiffnesses, the displacement values obtained with the proposed method are very close to those of the Newmark method.

### 5.3. Comparison of the Results with Different Period Ratios.

The frequency content of these records was characterized by the mean period ( $T_m$ ), defined as

$$\mathbf{T}_m = \frac{\sum_i \mathbf{C}_i^2 (\mathbf{i}/f_i)}{\sum_i \mathbf{C}_i^2}, \quad (38)$$

where  $C_i$  represents the Fourier amplitudes of the entire accelerogram and  $f_i$  represents the discrete Fourier transform frequencies between 0.25 and 20 Hz [24]. The

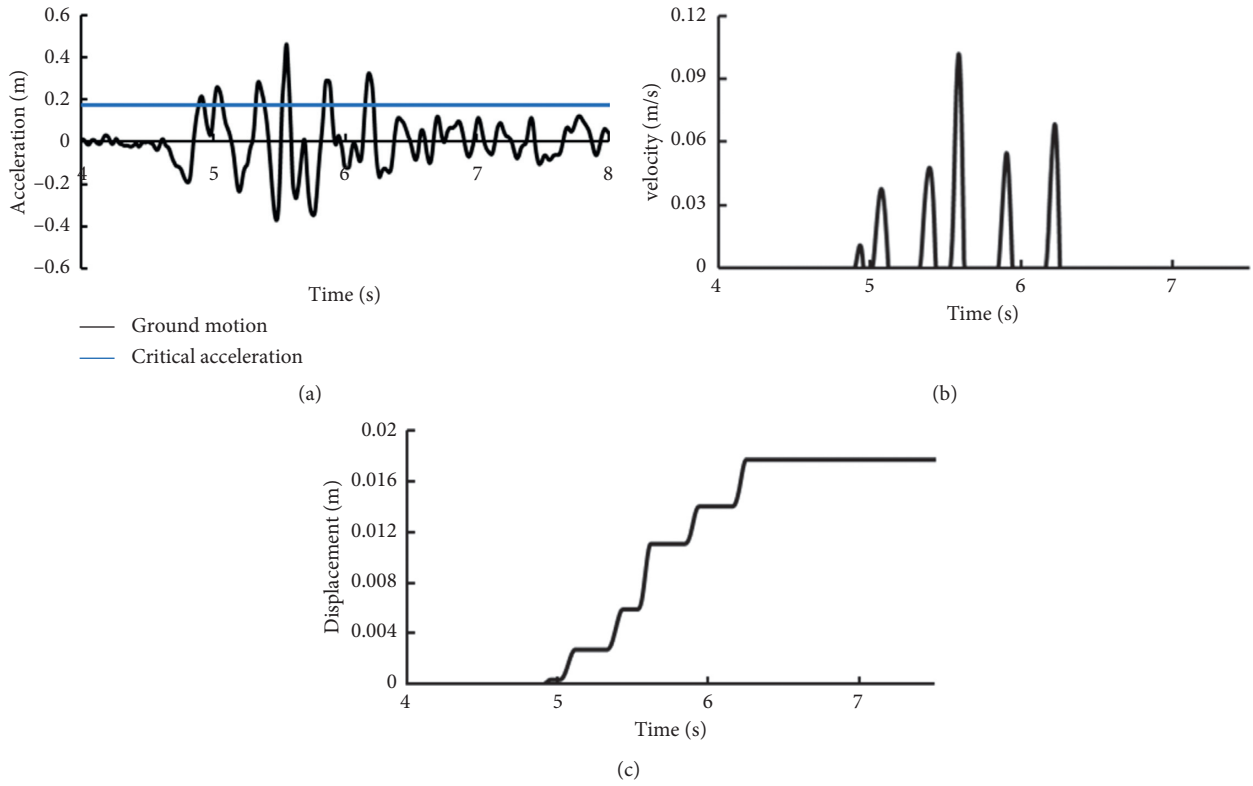


FIGURE 4: The results of the rigid block calculated by proposed method. (a) The ground motion; (b) the velocity of the sliding body; (c) the cumulative displacement.

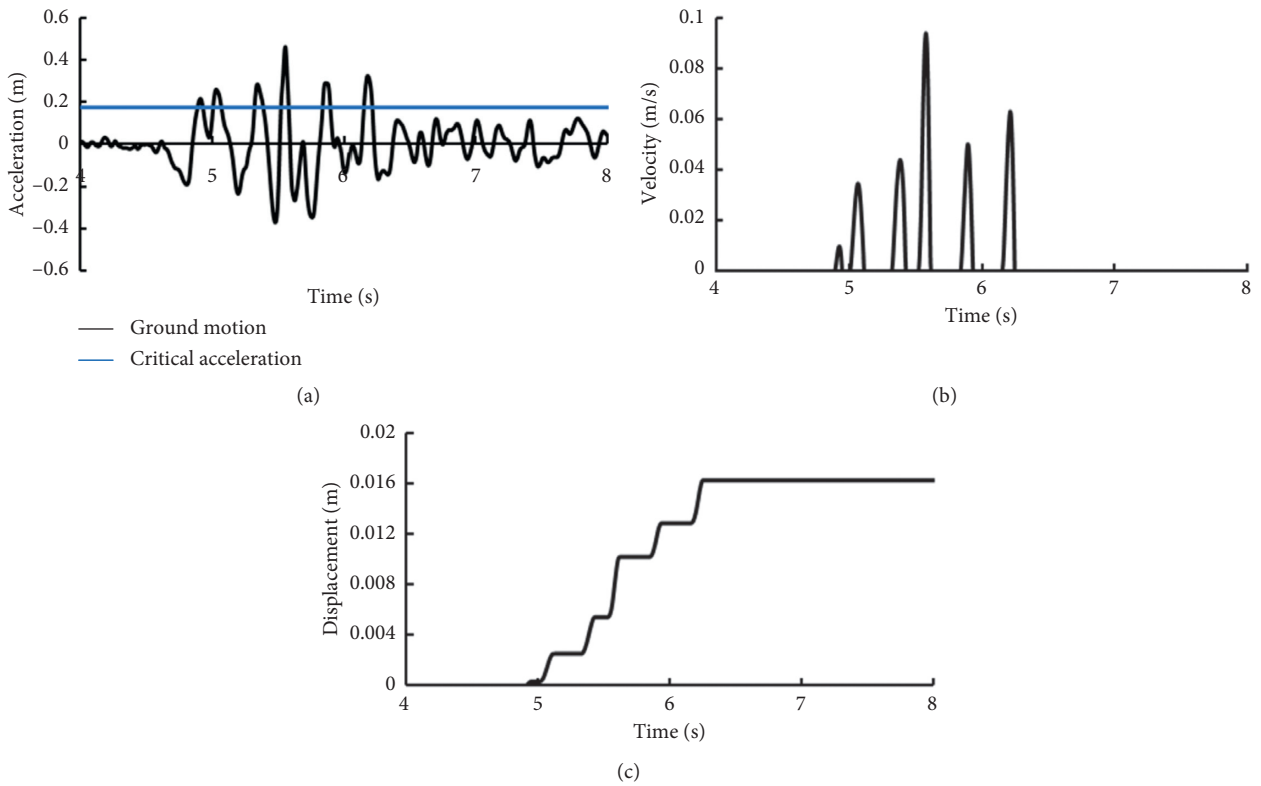


FIGURE 5: The results of the rigid block calculated by Newmark method. (a) The ground motion; (b) the velocity of the sliding body; (c) the cumulative displacement.

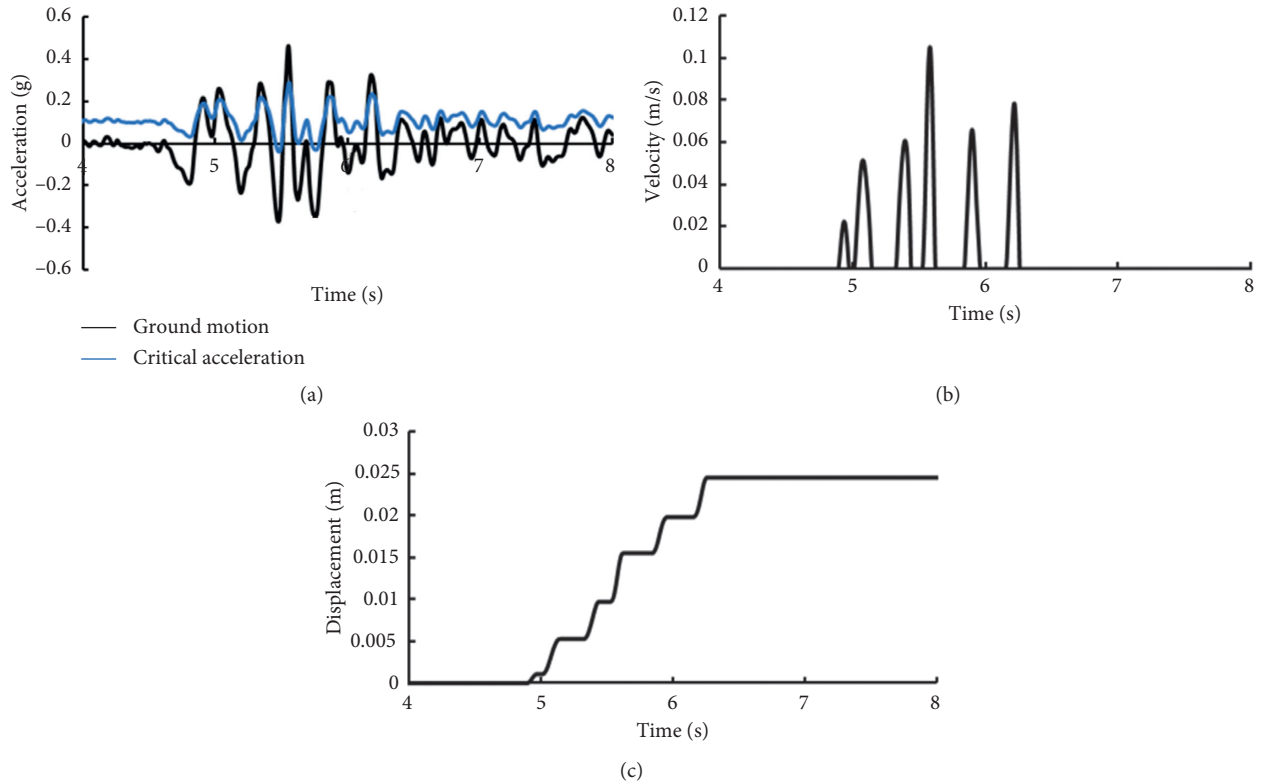


FIGURE 6: The results of the proposed method. (a) The ground motion; (b) the velocity of the sliding body; (c) the cumulative displacement.

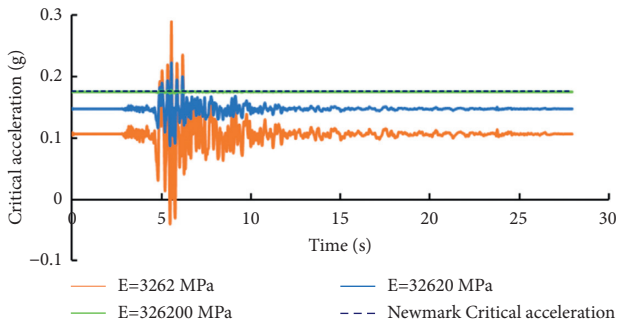


FIGURE 7: Comparisons of the critical acceleration.

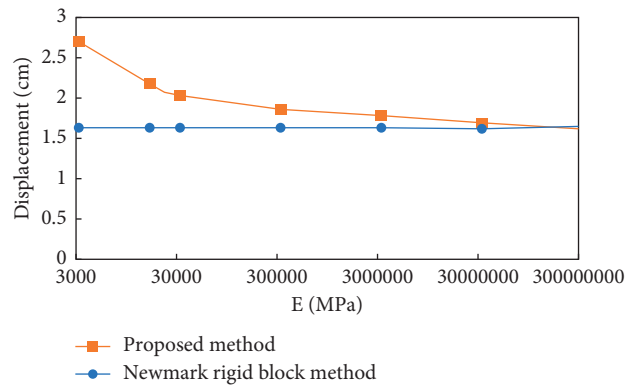


FIGURE 8: Comparisons of the sliding displacement variation with increasing stiffness.

fundamental period of the earth system is estimated as  $T_s = 4H/V_s$ . The period ratios of  $T_s/T_m$  will be used to present the results in this paper. The recorded ground motion of the Pacoima Dam Downstream record from the 1994 Northridge earthquake is used as the input motion (Figure 9), which is used in the Newmark rigid block method, the proposed rigid block model, and the flexible model.  $T_m$  of the record is equal to 0.47 s, and  $T_s$  is varied by changing the height of the systems. The shear-wave velocity of the soil is 2016 m/s, and the damping is considered as 15%. The parameters include a unit weight of 20 kN/m<sup>3</sup>, a slope angle of 15°, and a friction angle of 17.4°.

Figure 10 presents the variation in the proposed and Newmark displacement with period ratio,  $T_s/T_m$ . The results show that, for the rigid block, the proposed method has a slightly larger one than the Newmark method

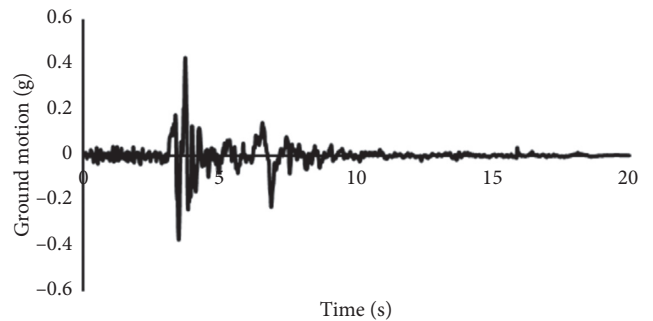


FIGURE 9: The ground motion of the Pacoima Dam Downstream record from the 1994 Northridge earthquake.

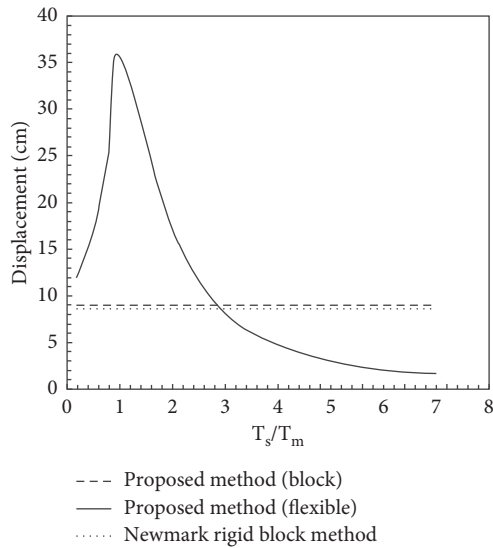


FIGURE 10: Variation in the sliding displacement with  $T_s/T_m$  for the Newmark method and the proposed method using the Pacoima Dam Downstream record.

because the proposed method considered the relative displacement. At small values of  $T_s/T_m$ , the flexible system analysis results of the displacement are larger than the results of the rigid block model. At larger values of  $T_s/T_m$ , the rigid block model is more conservative than the flexible system. In addition, the flexible system analysis never allows the full response to develop because as the response increases, sliding is initiated and is somewhat isolated from the base of the system.

## 6. Conclusion

The proposed method of the rigid block model has the same critical acceleration as the Newmark method. However, because the proposed method considers the relative displacement in the rigid block model, the proposed method is more conservative than the Newmark method. For the flexible system, the stiffness is increased in the proposed analysis, and when the stiffness tends to infinity, the results of the proposed method are close to those of the Newmark method. The proposed method is also compared with the Newmark method with the period ratio  $T_s/T_m$ . At small values of  $T_s/T_m$ , the flexible system analysis results of the displacement are larger than those of the rigid block model. At larger values of  $T_s/T_m$ , the rigid block model is more conservative than the flexible system.

## Data Availability

The data used to support the findings of this study are available from the corresponding author upon request.

## Conflicts of Interest

The authors declare that they have no conflicts of interest.

## Acknowledgments

This work was supported in part by the National Natural Science Foundation of China (Grant nos. 41977252 and 41572291), the Sichuan Provincial Youth Science and Technology Innovation Team Special Projects of China (Grant no. 2017TD0018), the Team Project of Independent Research of SKLGP (Grant no. SKLGP2020Z001), and the State Key Laboratory of Geohazard Prevention and Geo-environment Protection of the Chengdu University of Technology Open Fund (Grant nos. SKLGP2019K010 and SKLGP2020K015).

## References

- [1] D. K. Keefer, "Landslides caused by earthquakes," *The Geological Society of America Bulletin*, vol. 95, p. 406, 1984.
- [2] R. W. Jibson, E. L. Harp, W. Schulz, and D. K. Keefer, "Large rock avalanches triggered by the m 7.9 denali fault, Alaska, earthquake of 3 november 2002," *Engineering Geology*, vol. 83, pp. 144–160, 2006.
- [3] R. W. Jibson, E. L. Harp, and J. A. Michael, "A method for producing digital probabilistic seismic landslide hazard maps," *Engineering Geology*, vol. 58, no. 3-4, pp. 271–289, 2000.
- [4] E. M. Rathje and G. Antonakos, "A unified model for predicting earthquake-induced sliding displacements of rigid and flexible slopes," *Engineering Geology*, vol. 122, pp. 51–60, 2011.
- [5] K. Terzaghi, *Mechanisms of Landslides*, *Engineering Geology (Berdey) Volume*, Geological Society of America, Boulder, CO, USA, 1950.
- [6] R. W. Day, *Geotechnical Earthquake Engineering*, McGraw-Hill, New York, NY, USA, 1996.
- [7] R. Ohno, S. Niwa, H. Iwata, and S. Ozawa, *An Examination of the Stability of an Earthquake-Induced Landslide and Landslide Dam*, Springer, Berlin, Germany, 2013.
- [8] R. C. Wilson and D. K. Keefer, "Dynamic analysis of a slope failure from the 6 august 1979 coyote lake, California, earthquake," *Bulletin of the Seismological Society of America*, vol. 73, pp. 863–877, 1983.
- [9] H. B. Seed, K. L. Lee, and I. M. Idriss, "Analysis of sheffield dam failure," *Journal of the Soil Mechanics and Foundations Division*, vol. 95, 1969.
- [10] H. B. Seed, K. L. Lee, I. M. Idriss, and F. I. Makdisi, "The slides in the san fernando dams during the earthquake of february 9, 1971," *Journal of Geotechnical and Geoenvironmental Engineering*, vol. 101, 1975.
- [11] N. M. Newmark, "Effects of earthquakes on dams and embankments," *Geotechnique*, vol. 15, pp. 139–160, 1965.
- [12] F. I. Makdisi and H. B. Seed, "Simplified procedure for estimating dam and embankment earthquake-induced deformations," *Journal of Geotechnical and Geoenvironmental Engineering*, vol. 104, 1978.
- [13] E. M. Rathje and J. D. Bray, "Nonlinear coupled seismic sliding analysis of earth structures," *Journal of Geotechnical and Geoenvironmental Engineering*, vol. 126, pp. 1002–1014, 2000.
- [14] N. N. Ambraseys and J. M. Menu, "Earthquake-induced ground displacements," *Earthquake Engineering and Structural Dynamics*, vol. 16, no. 7, pp. 985–1006, 1988.
- [15] S. W. Qi, "Evaluation of the permanent displacement of rock mass slope considering deterioration of slide surface during

- earthquake,” *Chinese Journal of Geotechnical Engineering*, vol. 29, no. 3, pp. 452–457, 2007.
- [16] H. Zafarani and M. Soghrat, “Simulation of ground motion in the zagros region of Iran using the specific barrier model and the stochastic method,” *Bulletin of the Seismological Society of America*, vol. 102, pp. 2031–2045, 2012.
- [17] Y. Jafarian, R. Vakili, A. S. Abdollahi, and M. H. Baziar, “Simplified soil liquefaction assessment based on cumulative kinetic energy density: attenuation law and probabilistic analysis,” *International Journal of Geomechanics*, vol. 14, pp. 267–281, 2013.
- [18] S. Dong, W. Feng, Y. Yin, R. Hu, H. Dai, and G. Zhang, “Calculating the permanent displacement of a rock slope based on the shear characteristics of a structural plane under cyclic loading,” *Rock Mechanics and Rock Engineering*, vol. 53, pp. 4583–4598, 2020.
- [19] R. W. Jibson, “Predicting earthquake-induced landslide displacements using newmark’s sliding block analysis,” *Transportation Research Record*, vol. 1411, pp. 9–17, 1993.
- [20] L. Kramer, *Geotechnical Earthquake Engineering*, Prentice-Hall, Hoboken, NJ, USA, 1996.
- [21] E. M. Rathje and J. D. Bray, “An examination of simplified earthquake-induced displacement procedures for earth structures,” *Canadian Geotechnical Journal*, vol. 36, pp. 72–87, 1999.
- [22] N. Mostaghel and J. Tanbakuchi, “Response of sliding structures to earthquake support motion,” *Earthquake Engineering & Structural Dynamics*, vol. 11, pp. 729–748, 1983.
- [23] J. D. Bray and T. Travararou, “Simplified procedure for estimating earthquake-induced deviatoric slope displacements,” *Journal of Geotechnical and Geoenvironmental Engineering*, vol. 133, no. 4, pp. 381–392, 2007.
- [24] J. D. Bray and E. M. Rathje, “Earthquake-induced displacements of solid-waste landfills,” *Journal of Geotechnical and Geoenvironmental Engineering*, vol. 124, no. 3, pp. 242–253, 1998.